CHAPTER 125

WAVE ACTION ON AND IN PERMEABLE STRUCTURES

M.R.A. van Gent[1], P. Tönjes[2], H.A.H. Petit[3] and P. van den Bosch[3]

ABSTRACT: A numerical model that can simulate plunging waves on permeable structures is described. The 'Volume Of Fluid' method is used to solve the two-dimensional (2D-V) incompressible Navier-Stokes equations. After implementation of porous media flow for applications with permeable structures, the model has been verified by using several analytical solutions and by comparisons with physical model tests to study breaking waves on and inside permeable structures.

INTRODUCTION

Wave motion on permeable structures has often been studied using physical models. Small-scale physical modelling is influenced by scale effects while large-scale modelling is relatively expensive. Apart from this, measurements within breaking waves can be very complex. Therefore, numerical models simulating individual breaking waves are valuable design and research tools for studying wave motion on and inside coastal structures.

The description of breaking waves, the interaction with the porous part of permeable structures and the verification of the implementation of the most important phenomena involved, require a considerable amount of research of which some aspects are treated here. The numerical model described here (SKYLLA) was verified for breaking waves over a submerged bar, described in Van Gent et al. (1994-a). Other research concerning this numerical model, including the in- and outflow boundaries as well as the description of impermeable slopes were presented by Van der Meer et al. (1992) and Petit et al. (1994-b).

After a description of the numerical model and the method to solve the Navier-Stokes equations, adapted Navier-Stokes equations for porous media flow will be

1) Delft University of Technology, Department of Civil Engineering, P.O.Box 5048, 2600 GA Delft. 2) Rijkswaterstaat, Road and Hydraulic Engineering Division, P.O.Box 5044, 2600 GA Delft. 3) Delft Hydraulics, P.O.Box 152, 8300 AD Emmeloord, The Netherlands.

given. The implementation of these are validated using both analytical solutions and physical model tests. The physical model tests are performed with a Berm breakwater where surface elevations, velocities and pore-pressures are measured.

NUMERICAL MODEL

Several models to simulate breaking waves have been made. For instance Vinje and Brevig (1981) used a potential flow model and modelled a plunging wave until the overturning wave hits the trough water. Sakai *et al.* (1986) applied the MAC-method to simulate breaking waves. Here, the 'Volume of Fluid' (VOF) method by Hirt and Nichols (1981) is used to solve the Navier-Stokes equations in two dimensions. This powerful method enables simulation of complex flow patterns including those where the free surface can become multiply connected. To achieve this, the treatment at the surface based on the adapted flux-method known as FLAIR by Ashgriz and Poo (1991), has been improved. Figure 1 shows that an overturning wave on an impermeable slope can be simulated by applying the Navier-Stokes equations solved using the VOF-method.
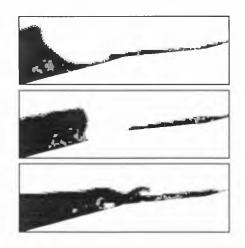

Fig.1   *Simulation of a breaking wave on an impermeable dike with a berm.*

The VOF-method is a method where for each cell the fluid fraction can vary between zero (empty) and one (full). Fluid fractions are transported between each cell and its surrounding cells. In Figure 2 the principle of the method is shown for the transport between two neighbouring cells. Based on the two fluid fractions of two neighbouring cells, a 'local surface' can be constructed. By using the velocity

and the time-step (varied based on the instantaneous stability and accuracy criteria), a part of the fluid is transported between these two cells. In the numerical model this is done using a non-equidistant staggered grid.
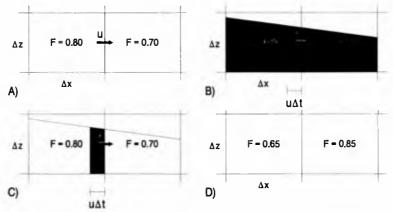

Fig.2   *Transport of fluid based on the VOF-method.*

The velocity as used in the VOF-method is obtained from the discretisation of the Navier-Stokes equations. At impermeable slopes and at the free surface not all velocities necessary to discretise the equations are within the fluid domain. Figure 3 shows the required velocities for discretisation inside the fluid (A) and near the free surface (B). Boundary conditions are required to fill the lack of information at the free surface. For instance one can assume no gradient in the velocities at the surface or that the flow is irrotational at the surface.
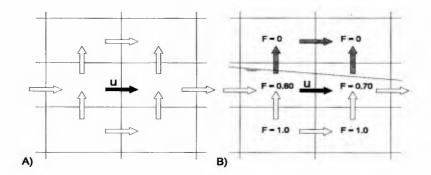

Fig.3   *Required information for discretisation of horizontal velocities.*

Two open weakly-reflecting boundaries can be used at which regular wave trains can both be generated and absorbed. The incoming non-linear waves are based on the theory by Rienecker and Fenton (1981). The boundary for impermeable slopes are defined on sub-grid level which means that the slope can intersect cells (no 'stair-case' slope). At impermeable slopes no-slip or free-slip boundaries can be applied. In Van Gent *et al.* (1994-a) two weakly-reflecting boundaries were applied for wave breaking over a submerged bar schematised with a free-slip boundary. The comparison of these computed breaking waves with video images showed that plunging occurs at the same position as in the physical model tests. Although the decrease in wave height occurs somewhat quicker in the numerical model than in reality, the height of the transmitted wave is accurate. Here, after implementation of porous media flow, breaking waves on permeable structures will be verified.

IMPLEMENTATION OF POROUS MEDIA FLOW

The VOF-method can also be applied for solving the wave motion inside permeable structures. The momentum equations, however, are different from those for the external wave motion. The Navier-Stokes/Reynolds equations for the external wave motion read:

$$\frac{\partial u}{\partial t} + \frac{\partial u^2}{\partial x} + \frac{\partial u w}{\partial z} + \frac{1}{\rho_w}\frac{\partial p}{\partial x} - \nu_t\left(\frac{\partial^2 u}{\partial x^2} + \frac{\partial^2 u}{\partial z^2}\right) + g_x = 0 \qquad (1)$$

$$\frac{\partial w}{\partial t} + \frac{\partial u w}{\partial x} + \frac{\partial w^2}{\partial z} + \frac{1}{\rho_w}\frac{\partial p}{\partial z} - \nu_t\left(\frac{\partial^2 w}{\partial x^2} + \frac{\partial^2 w}{\partial z^2}\right) + g_z = 0 \qquad (2)$$

where u and w are the velocities in the x and z direction respectively and ν_t the eddy-viscosity for which a constant value will be used. Together with conservation of mass ($\partial u/\partial x + \partial w/\partial z = 0$), which is satisfied by solving the Poisson equation, and boundary conditions, the VOF-method can then be applied yielding the external wave motion. For the internal wave motion adapted Navier-Stokes equations were derived (see Van Gent, 1991):

$$\frac{1+c_A}{n}\frac{\partial u}{\partial t} + \frac{1}{n^2}\left(\frac{\partial u^2}{\partial x} + \frac{\partial u w}{\partial z}\right) + \frac{1}{\rho_w}\frac{\partial p}{\partial x} + g a u + g b u \sqrt{(u^2+w^2)} + g_x = 0 \qquad (3)$$

$$\frac{1+c_A}{n}\frac{\partial w}{\partial t} + \frac{1}{n^2}\left(\frac{\partial u w}{\partial x} + \frac{\partial w^2}{\partial z}\right) + \frac{1}{\rho_w}\frac{\partial p}{\partial z} + g a w + g b w \sqrt{(u^2+w^2)} + g_z = 0 \qquad (4)$$

where u and w are both filter-velocities, a and b are dimensional friction coefficients and c_A is a coefficient to take the phenomenon *added mass* into account. Because filter/discharge velocities are used, the procedure to transport mass between the

cells, the VOF-method, does not require any adaptation. The discretisation (partial upwind scheme) and stability criteria are described in Van Gent *et al.* (1994-b). In the computational domain numerous regions with different properties can be selected and awarded a certain porosity and stone diameter. The permeable slopes are not, like for impermeable slopes, defined on sub-grid level which means that the properties cannot be varied within one cell. Permeable slopes can also be combined with impermeable regions. This implementation of permeable parts in this two-dimensional model, therefore, enables applications with breaking waves and other complex flow patterns for a very wide range of structure types. Here, some validation tests will be discussed. For some other applications see for instance Van Gent and Petit (1994).

VALIDATION WITH ANALYTICAL SOLUTIONS

Several verifications of the implementation of porous media flow have been performed. Before the wave motion on and inside a permeable structure is verified using physical model tests, three comparisons with analytical solutions are carried out. The first case concerns a layer of water with a thickness L that is initially positioned above a dry permeable part, see Figure 4. At $t=0$, the layer of water starts entering the permeable part. For this simplified case of uniform flow entering a permeable part $(-L < x_0 < 0)$, the Navier-Stokes equations reduce to a set of one dimensional differential equations (Van Gent *et al.*, 1994-b) where u is the filter-velocity, n the porosity and x_0 the position of the free surface, at $t=0$, $x_0=-L$:

$$\frac{du}{dt} = \frac{-\frac{g}{n}(L+x_0)(au+bu^2-1)-(\frac{1}{n^2}-1)u^2-gx_0}{\frac{L+x_0}{n^2}-x_0} \tag{5}$$

With $dx_0/dt = u$, this set of differential equations was solved using a fourth-order Runge-Kutta method with $\Delta t = 0.005 \ s$ and $\Delta x = 0.05 \ m$ while for the constants L, n, g, a, b the values $0.5 \ m$, 0.5, $4 \ m/s^2$, $0 \ s/m$ and $16.9 \ s^2/m^2$ were used respectively (for g, $4 \ m/s^2$ is taken instead of $9.81 \ m/s^2$ to exaggerate the local maximum in Figure 4). After the layer has entered the permeable part, the differential equation reduces to: $du/dt=ng(1-au-bu^2)$ for which an analytical solution was found:

$$u(t) = \left(u_1 - u_2 \frac{u(t_0)-u_1}{u(t_0)-u_2} e^{-bng(u_1-u_2)(t-t_0)}\right) \Big/ \left(1 - \frac{u(t_0)-u_1}{u(t_0)-u_2} e^{-bng(u_1-u_2)(t-t_0)}\right) \tag{6}$$

where $u_1=-a/2b+\sqrt{(a^2+4b)}/2b$, $u_2=-a/2b-\sqrt{(a^2+4b)}/2b$ and $u(t_0)$ is the initial velocity at $t=t_0$ where t_0 is the moment at which the whole layer of water has
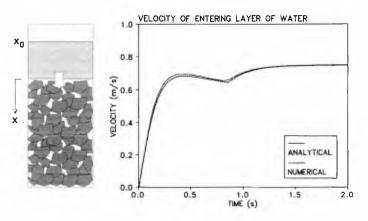
Fig. 4   *Comparison of numerical model results with solutions of simplified differential equations for the velocity of a layer of water entering a porous block.*
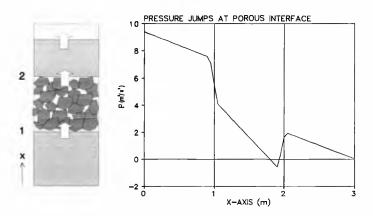

Fig. 5   *Calculated pressure jumps at the interfaces of a porous block with a steady flow.*

entered the permeable part. Figure 4 shows the comparison of the numerical results and these solutions. At $t=0$, the velocity is zero, at $t=0.435$ s a local maximum of $u=0.6848$ m/s occurs and at $t=0.850$ s (t_0) the layer has entered the permeable part after which the velocity rapidly converges to the velocity 0.75 m/s. The difference between the numerical model results and the solutions of the set of simplified differential equations reaches a maximum of 0.0129 m/s at $t=0.4$ s. As shown in Figure 4, the phenomenon is reproduced with good result.

A second verification concerns the flow through a saturated permeable block, see Figure 5. At $x=0$ a constant inflow with a velocity of 1 m/s is produced, between $x=1$ m and $x=2$ m a saturated permeable block is positioned. The pressure jumps at the porous interfaces ($x=1$ m and $x=2$ m) can be determined analytically. Integrating the momentum equation for a uniform flow in the x-direction yields:

$$P\ (x_2+\delta x)\ -\ P\ (x_2-\delta x)\ =$$
$$\left(\frac{1}{n^2}\ -\ 1\right) u^2\ -\ \delta x \left(g\ (au+bu^2+2)\ +\ (1+\frac{1+c_A}{n})\ \frac{\partial u}{\partial t}\ \right) \qquad (7)$$

where x_2 is the position of the outflow boundary ($x=2$ m). The same procedure can be used at the inflow boundary ($x=1$ m). The pressure jump is then equal to the one at the inflow boundary, except for the sign. Outside the stone the pressure is determined by $\partial P/\partial x=-g$ while inside the stone the pressure gradient can be assessed through $\partial P/\partial x=-g(au+bu^2+1)$. In Figure 5 the comparison between the analytical solution and the numerical results is shown. Some arbitrary values for the constants n, a, b and g were used (0.5, 1 s/m, 0.75 s^2/m^2 and 2 m/s^2 respectively). Because in the numerical model the pressure jumps are simulated in steps of $3\Delta x$, $\delta x=3/2\Delta x$ is used in the analytical solution (Equation 7) for comparison with the numerical model results. The pressure jumps by the analytical solution and the numerical model results were 2.4375 m^2/s^2 and 2.5065 m^2/s^2 respectively. This comparison is again rather good. For $\delta x \downarrow 0$, the real analytical solution gives 3 m^2/s^2 to which the numerical model results will come close for smaller values of Δx.
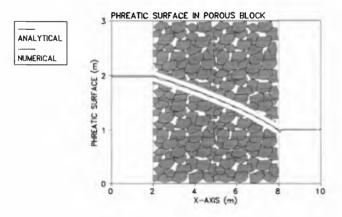

Fig.6 *Comparison of numerically computed phreatic surface and an analytical solution.*

A third analytical solution has been compared with numerical model results. Now, a stationary flow through a rectangular block with only linear porous friction

($b=0$) has been examined. Neglecting convection and assuming hydrostatic pressures and uniform flow over the depth, the solution for the phreatic surface is determined by $h(x')=\sqrt{(H_1^2-x'/L(H_1^2-H_2^2))}$ where H_1 is the free surface level at the inflow boundary (left in Figure 6), H_2 is the free surface level at the outflow boundary and L the length of the permeable block (for Figure 6: $x'=x-2$). Some arbitrary values for the constants n, a, L and g were used (0.2, 4.0 s/m, 6.0 m and 10 m/s^2 respectively). The levels H_1 and H_2 where 2.0 m and 1.0 m respectively. In the numerical computation, $\Delta x=0.1$ m has been used. The phreatic level was defined as the level where in the computation 50% of the cell was filled with water ($F=0.5$). Differences between both phreatic surfaces at $x=2$, 4, 6 and 8 m in Figure 6 were 0.0233, 0.0206, 0.0105 and 0.0234 m, respectively.

VALIDATION WITH PHYSICAL MODEL TESTS

By means of the numerical model complex phenomena such as scale effects, wave transmission, the effects of non-stationary porous media flow, added mass and forces on stones can be studied. However, a verification with physical models must be performed first.

Non-stationary porous media flow tests have been performed in a U-tube tunnel. These measurements resulted in expressions for the porous media flow friction-coefficients a, b and c_A in Equations 3 and 4, see Van Gent (1994). For the dimensional coefficients a and b, theoretically derived expressions are used: $a=\alpha\cdot(1-n)^2/n^3\cdot\nu/gD_{n50}^2$, $b=\beta\cdot(1-n)/n^3\cdot\nu/gD_{n50}$ and $c_A=\gamma\cdot(1-n)/n$. The physical model tests showed a dependency of β on the flow field, accounted for by including a dependency of β on the KC-number, $\beta=\beta_c(1+7.5/KC)$, where $KC=\hat{U}T/nD_{n50}$ and $\beta_c=1.1$. In the computations with the numerical model this has been included by estimating a representative filter-velocity $\hat{U}$ beforehand and using the wave period for T.
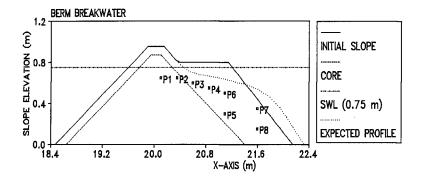

Fig.7   *Cross-section of the Berm breakwater in experimental set-up.*

A second series of physical model tests was performed to verify the numerical model. A small-scale model of a Berm breakwater was used for this purpose. Figure 7 shows a sketch of the experimental set-up with the initially horizontal berm at a level of 0.80 m, the still water level being 0.75 m. All slopes were $1:1.5$ except for the submerged seaward slope which was $1:1.25$. The size of the stone material was $D_{n50}=0.0266$ m in the cover layer and $D_{n50}=0.0175$ m in the core. The porosity of the two permeable parts were measured in situ, both giving $n=0.417$. Reshaping the seaward profile was achieved by four series of 1000 regular waves. After the last series, with the largest waves, the seaward profile was reshaped while the crest was heightened from 0.95 m to 1.00 m. Several series of regular waves were used to study the flow field. No reshaping took place during these tests. The flow field was recorded using a video, electro-magnetic flow meters (EMF), wave gauges and pressure transducers. The positions of the pressure transducers are indicated in Figure 7.

Surface elevations above the seaward slope were determined at ten points of time within a wave cycle for four series of regular waves: $H=0.119$ m, $T=1.5$ s; $H=0.230$ m, $T=1.5$ s; $H=0.112$ m, $T=2.1$ s and $H=0.217$ m, $T=2.1$ s. The computational domain in the numerical model started at 4 m in front of the toe of the reshaped structure where the waves were generated at this weakly reflecting boundary by applying the method by Rienecker and Fenton (1981) using 16 Fourier-components. This method was adapted to deal with reflected waves as described in Petit et al. (1994-a). No net transport was allowed through this boundary. At the landward boundary again a weakly reflecting boundary was positioned at 1.5 m behind the crest of the structure. In x and z-direction, 270 and 80 computational cells were used respectively. The computations were performed with a constant viscosity $\nu_t=0.005$ m^2/s. In the discretisation of the equations an up-wind fraction of 0.2 was used. Surface elevations were defined at positions of cells which were filled with fluid for 50%. After an adjustment time of six to eight waves to obtain a periodic computation, data was used for comparison with the measured properties.

Figure 8 shows comparisons of surface elevations for ten points of time for two wave conditions with a wave period of 1.5 s (five surface profiles per graph with 0.15 s in between two profiles). Only the surface elevations above the berm, where the waves are breaking, are shown since in the section in front of the structure only minor differences in wave height occur. Also for the two wave conditions with a wave period of 2.1 s, as shown in Figure 9 (0.21 s in between two profiles), the comparisons for the five profiles in the first half of each wave cycle show good agreement (upper graph for each wave condition). In the second half of each wave cycle (lower graph for each wave condition) considerable air-entrapment occurs for the two highest waves. In the figures with measured surface elevations the position of entrapped air is indicated by the area in between the two lines of each surface profile. The comparisons with the computed results become rather complex in this part since the exact position of the free surface is not clear. However, the comparisons indicate that the decrease in wave height above the berm faster occurs
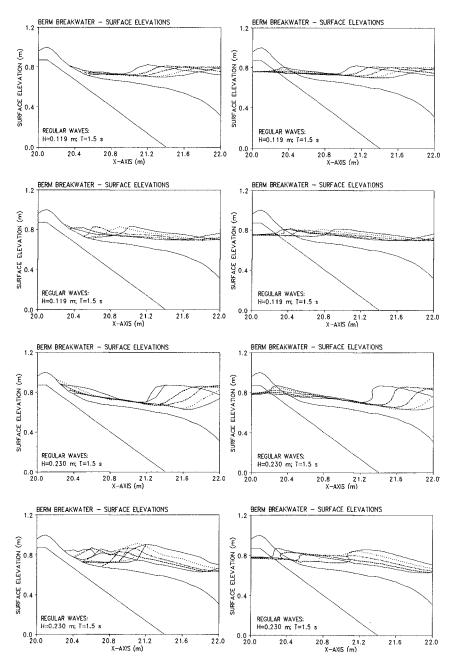
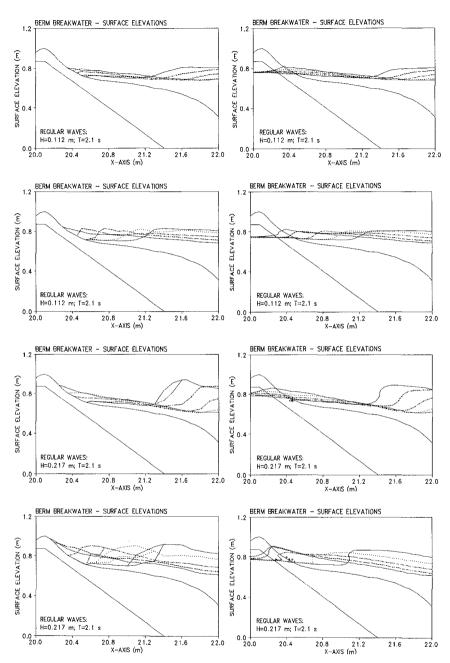**Fig. 8**   *Comparison of measured (left) and computed (right) surface elevations.*

Fig. 9 *Comparison of measured (left) and computed (right) surface elevations.*

in the computation than observed from the measurements. It seems as if this overestimated reduction in wave height, possibly due to a too large dissipation, leads to an underestimation of the run-up levels. For the two wave conditions with smaller waves, the comparisons are also rather good in the second half of the wave cycle.

For all four wave conditions $H=0.119$ m, $T=1.5$ s; $H=0.230$ m, $T=1.5$ s; $H=0.112$ m, $T=2.1$ s; $H=0.217$ m, $T=2.1$ s, the computed run-up levels are too low compared with the measured run-up levels: 0.07 vs. 0.10; 0.14 vs. 0.21; 0.08 vs. 0.11 and 0.18 vs. 0.27 m, respectively. All these values are relative to the average water levels in front of the structure during testing. The choice to define the surface elevations at the positions of cells that are filled with water for 50% instead of another percentage, might influence the computed run-up levels slightly. If for this definition positions of cells that are filled with water for 10% are regarded as surface elevations, the computed run-up levels might increase but not so much that they would fit to the measured run-up levels. The dissipation in the computedbreaking process, by the description of the physical processes or by numerical dissipation, is assumed to cause these underestimated run-up levels.

Comparisons between measured and computed velocities were made. Because of air-entrainment the position closest to the crest without this difficulty was at $x=21.6$ m, $z=0.65$ m. For three waves the comparisons for both the horizontal (u) and the vertical (w) velocities are shown in Figure 10. The comparison for the fourth wave $(H=0.217$ m and $T=2.1$ $s)$ was not possible because in the physical model this position was dry for some period within a wave cycle causing severe disturbance of the measured signal. The comparisons for the other three waves show accurate results for both the horizontal and vertical velocities.
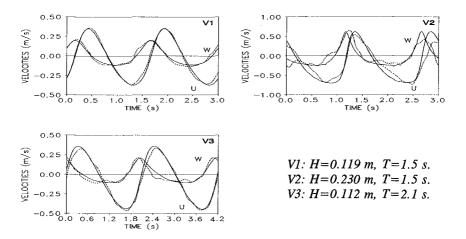

V1: $H=0.119$ m, $T=1.5$ s.
V2: $H=0.230$ m, $T=1.5$ s.
V3: $H=0.112$ m, $T=2.1$ s.

Fig.10   *Comparison of velocities at $x=21.6$ m and $z=0.65$ m; measured (dashed) and computed (lines).*
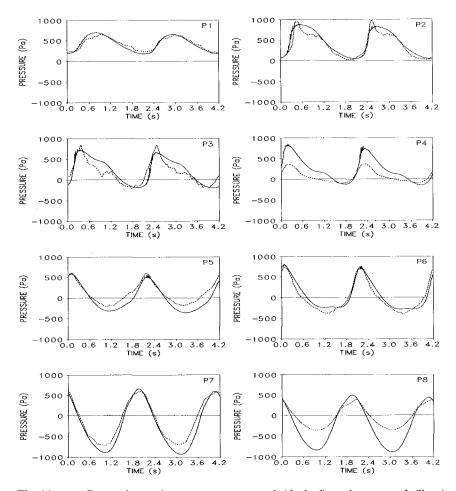
Fig.11   *Comparison of pressures; measured (dashed) and computed (lines), H=0.217 m, T=2.1 s.*

Also comparisons between measured and computed pressures were made. Figure 11 shows the signals from the eight transducers and the computed pressures at the same positions. The positions of these transducers are shown in Figure 7. Transducer *P4* is positioned in between the transducers *P3* and *P6*. The recorded pressures by transducer *P4*, however, clearly deviate from those recorded by *P3* and *P6*. Because no decisive physical explanation can be given for these low pressures, estimated to be roughly 50% of the expected pressures for all analysed wave conditions, the signals of transducer *P4* are highly questionable. The comparisons with the other transducers are fairly accurate except for those with transducer *P8*.

Both the internal set-up as recorded by transducer *P1* (average level) and the internal wave height are reproduced with a high accuracy. The computed signals at positions just below the breaking waves, transducers *P2*, *P3* and *P6*, also show good correspondence with the measured signals although these measured signals show more higher-order fluctuations.

CONCLUDING REMARKS

A numerical model solving the two-dimensional Navier-Stokes equations for simulating normally incident waves, including breaking waves, has been extended with porous media flow. The implementation of the combined external and internal wave motion on and inside permeable structures was successful as shown by comparisons with both analytical solutions and physical model tests. The model, now capable of providing a detailed flow description of breaking waves on permeable structures, will, however, be improved by including more sophisticated modelling of air-extrusion and turbulence. Furthermore, irregular waves will be implemented.

ACKNOWLEDGEMENTS

REFERENCES

Ashgriz, N. and J.Y. Poo (1991), *FLAIR: Flux line-segment model for advection and interface reconstruction*, J. of Comp. Physics Vol.39, pp.449-468.

Gent, M.R.A. van (1991), *Formulae to describe porous flow*, Report MAST-G6 Coastal Structures, project 1 and Communications on Hydraulic and Geotechnical Engineering, ISSN 0169-6548 No.92-2, Delft University of Technology.

Gent, M.R.A. van (1994), *Permeability measurements for the modelling of wave action on and in porous structures*, Proc. Coastal Dynamics'94, pp.671-685, Barcelona.

Gent, M.R.A. van, J.P. de Waal, H.A.H. Petit and P. van den Bosch (1994-a), *SKYLLA: Wave motion in and on coastal structures; Verification of wave kinematics of waves breaking on an offshore bar*, Delft Hydraulics Report H1780.

Gent, M.R.A. van, H.A.H. Petit and P. van den Bosch (1994-b), *SKYLLA: Wave motion in and on coastal structures; Implementation and verification of flow on and in permeable structures*, DELFT HYDRAULICS Report H1780.

Gent, M.R.A. van, and H.A.H. Petit (1994), *Simulations of wave interaction with coastal structures*, Proc. Hydroinformatics'94, Vol.1, pp.141-146, IHE, Delft.

Hirt, C.W. and B.D. Nichols (1981), *Volume of fluid method for the dynamics of free boundaries*, J. of Comp. Physics Vol.39, pp.201-225.

Meer, J.W. van der, H.A.H. Petit, P. van den Bosch, G. Klopman and R.D. Broekens (1992), *Numerical simulation of wave motion on and in coastal structures*, Proc. ICCE'92, Vol.2, pp.1772-1784, Venice.

Petit, H.A.H., P. van den Bosch and M.R.A. van Gent (1994-a), *SKYLLA: Wave motion in and on coastal structures; Implementation and verification of modified boundaries*, DELFT HYDRAULICS Report H1780.

Petit, H.A.H., P. van den Bosch and M.R.A. van Gent (1994-b), *SKYLLA: Wave motion in and on coastal structures; Implementation of impermeable slopes and overtopping-boundary conditions*, DELFT HYDRAULICS Report H1780.

Rienecker, M.M. and J.D. Fenton (1981), *A Fourier method for steady water waves*, J. of Fluid Mechanics, Vol.104, pp.119-137.

Sakai, T., T. Muzutani, H. Tanaka and Y. Tada (1986), *Vortex formation in plunging breaker*, Proc. ICCE'86, Vol.1, pp.711-723, Taipei.

Vinje, T. and P. Brevig (1981), *Numerical simulation of breaking waves*, Advances in Water Resources, Vol.4, pp.77-82.